The role of andrographolide and its derivative in COVID-19 associated proteins and immune system

Yadu Nandan Dey
School of Pharmaceutical Technology, Adamas University, Kolkata-700126, West Bengal, India
Pukar Khanal
Department of Pharmacology and Toxicology, KLE College of Pharmacy, Belagavi, KLE Academy of Higher Education and Research (KAHER), Belagavi-590010, Karnataka, India
B. M. Patil
Department of Pharmacology and Toxicology, KLE College of Pharmacy, Belagavi, KLE Academy of Higher Education and Research (KAHER), Belagavi-590010, Karnataka, India
Manish M. Wanjari (manish.nriashrd@gmail.com)
Regional Ayurveda Research Institute for Drug Development, Gwalior-474009, Madhya Pradesh, India
https://orcid.org/0000-0003-0691-2652
Bhavana Srivastava
Regional Ayurveda Research Institute for Drug Development, Gwalior-474009, Madhya Pradesh, India
Shailendra S. Gurav
Goa College of Pharmacy, Panjim-403001, Goa, India
Sudesh N. Gaidhani
Central Council for Research in Ayurvedic Sciences, New Delhi-110058, India

Research Article

Keywords: Andrographolide, Andrographis paniculata, COVID-19, viral infection

Posted Date: June 18th, 2020

DOI: https://doi.org/10.21203/rs.3.rs-35800/v1

Abstract

Aim: In view of the strong immunomodulatory and antiviral activity of andrographolide and its derivative, the present study aimed to investigate the binding affinities of andrographolide and its derivative 14-deoxy-11,12-didehydroandrographolide with 3 major targets of COVID-19 i.e. 3CLpro, PLpro and spike protein followed by their gene-set enrichment analysis with special reference to immune modulation.

Materials and methods: SMILES of the compounds were retrieved from DigepPred database and the proteins identified were queried in STRING to evaluate the protein-protein interaction and modulated pathways were identified concerning the KEGG database. Drug-likeness and ADMET profiles were evaluated using MolSoft and admet SAR 2.0, respectively. Molecular docking was carried using autodock 4.0.

Results: Andrographolide and 14-Deoxy-11,12-didehydroandrographolide were predicted to have a high binding affinity with papain-like protease i.e. -6.7 kcal/mol and -6.5 kcal/mol, respectively while they interact with equal binding energies with 3clpro (-6.8 kcal/mol) and spike protein (-6.9 kcal/mol). Network pharmacology analysis revealed that both compounds modulated the immune system through the regulation of chemokine signaling pathway, Rap1 signaling pathway, Cytokine-cytokine receptor interaction, MAPK signaling pathway, NF-kappa B signaling pathway, Rassignaling pathway, p53 signaling pathway, HIF-1 signaling pathway, and Natural killer cell-mediated cytotoxicity. Although the 14-deoxy-11,12-didehydroandrographolide scored higher drug-likeness character, it showed less potency to interaction with targeted proteins of COVID-19.

Conclusion: The study suggests the strong interaction of the andrographolide and its derivative 14-deoxy-11,12-didehydroandrographolide against target proteins associated with COVID-19. Further, network pharmacology analysis elucidated the different pathways of immunomodulation. However, clinical research should be conducted to confirm the current findings.

Introduction

In December 2019, severe acute respiratory syndrome caused by novel severe acute respiratory syndrome novel coronavirus 2 (SARS-nCoV-2) (Zhu et al., 2020) emerged as a global pandemic from the Wuhan city, Hubei province, China. WHO designated this nSARS-CoV-2 infection as COVID-19. The nSARS-CoV-2 s a highly contagious virus that can be transmitted from person to person (Anonymous, 2020) leading to community transmission. COVID-19 has become a major global threat by influencing around 212 countries with almost half million death throughout the globe (Sinha et al., 2020a). It has majorly affected the subjects with comorbidty and low immunity who are suffering from infectious and non-infectious diseases (Opitz et al. 2010). Patients with COVID-19, especially those with severe pneumonia, showed substantially lower lymphocyte counts and severely ill patients exhibited reduction in CD4+ T cells, CD8+ T cells, and natural killer cells. (Huang et al., 2020; Wang et al., 2020) The higher plasma concentrations of a number of inflammatory cytokines such as IL-6 and tumor necrosis factor (TNF) were

observed in COVID-19 patients (Wan et al., 2020). The pathological findings in patients with COVID-19 showed that immune-mediated lung injury was involved in acute respiratory distress syndrome (ARDS) (Xu et al., 2020). These evidences suggested immune imbalance in COVID-19 and it was contemplated that the immune system modulaton can provide some prohylaxis and promising benefit against COVID-19 (Zhang et al., 2020). Hence, there is need to utilize the concept to identify the new therapeutic agent with immunomodulatory action as well as anti-viral property against the COVID- 19.

The effectiveness of treatment based on traditional medicinal plants has been reported during the 2003 SARS (Wen et al., 2011; Chen et al., 2008; Lin et al., 2008; Ryu et al., 2010). Therefore, the scientific community has already started studies on medicinal plants, based on their history and traditional uses, as plausible leads in the treatment of Covid-19 (Chikhale et al., 2020; Sinha et al., 2020a,b).

For thousands of years, medicinal plants have been playing important role in the management of multiple infectious and non-infectious diseases (Mahady 2005; Sofowora et al 2013; Bahmani et al 2015). Among them, *Andrographis paniculata* (Family: Acanthaceae) also called known as King of bitters and Indian Echinaceae, reserves its importance in the management of various infectious and non-infectious diseases (Wintachai et al., 2015; Pongtuluran and Rofaani 2015; Zhang and Tan 2000; Mopuri et al 2015). Further, it has been well studied for its potency as a modulator of the immune system (Pongtuluran and Rofaani 2015; Puri et al., 1993). Among the multiple phytoconstituents present in *Andrographis paniculata*, andrographolide (Mishra et al 2011) is a major bioactive which possesses its beneficial effect in multiple pathogenic conditions including immune booster role (Wang et al 2010). Further, two important databases i.e. ChEBI and PCIDB also record andrographolide as chief bioactive from *Andrographis paniculata.* Andrographolide and its derivatives exhibited strong immunomodulatory action (Churiyah et al., 2015; Puri et al., 1993) and is reported to have broad spectrum antiviral properties (Gupta et al., 2017). It was found effective against viral infections like dengue (Edwin et al., 2016), swine flu (Seniya et al 2014), hepatitis C (Lee et al., 2014), chickengunia (Wintachai et al., 2015), influenza (Chen et al., 2009), Epstein-Barr virus (EBV) (Lin et al. 2008) and herpes simplex virus 1 (HSV-1) (Wiart et al. 2005) in previous experimental studies.

Hence, the present study aimed to investigate the prospective potential andrographolide as a potent anti-viral agent by targeting three proteins of COVID-19 i.e. 3clpro, PLpro, and spike protein. Further, the study also evaluated the probable pathways to be regulated in enhancing the immune system. Since, during the mining of the andrographolide derivatives, we identified 14-deoxy-11,12-didehydroandrographolide as its derivative, hence the study also evaluated its potency for the anti-viral property against COVID-19 and the probably modulated pathways.

Materials And Methods

Prediction of targets

SMILES of 14-deoxy-11,12-didehydroandrographolide and andrographolidewas retrieved from the PubChem database (https://pubchem.ncbi.nlm.nih.gov/) and was queried for protein-based prediction in

DIGEP-Pred (Lagunin et al 2013) at a probable activity (Pa)>Probable inactivity (Pi).

Enrichment analysis

The list of up-and down-regulated proteins was queried in the STRING database (Szklarczyk et al 2017).The biological process, cell component, and molecular function were recorded. The modulated protein and their associated pathways were identified using the KEGG pathway database. The interaction between the compounds, their targets, and pathways was constructed using Cytoscape which was further analyzed using edge count.

In silico molecular docking

3D structure of 14-deoxy-11,12-didehydroandrographolide and andrographolide was retrieved from the PubChem database in .sdf format and converted into .pdb format using Discovery studio 2019. The ligand of each molecule was minimized using mmff94 forcefield and converted into .pdbqt format.Targets 3clpro (PDB: 6LU7), and PLpro (PDB: 4M0W) were retrieved from the RCSB database (https://www.rcsb.org/) which were in complexed with water molecules and hetero atoms; removed using discovery studio 2019 and saved in .pdb format. Spike protein of coronavirus washomology modeled target by using accession number AVP78042.1 as query sequence and PDB: 6VSB as a template using SWISS-MODEL (Schwede et al., 2003). Docking was carried using autodock4 (Morris et al., 2009). After docking ten different confirmations of ligand were obtained in which ligand possessing minimum binding energy was chosen to visualize the ligand-protein interaction using discovery studio 2019.

Calculation of drug-likeness and ADMET

Drug-likeness of the compound was calculated based on the Rule of five using Molsoft (https://molsoft.com/mprop/) by querying the SMILES of compounds. Further, absorption, distribution, metabolism, and excretion were calculated using admetSAR2.0 (Yang et al 2019).

Results

Prediction of targets

Andrographolide was predicted to regulate down-regulated 36 proteins in which 17 were down-regulated and 19 were upregulated. Likewise, 14-Deoxy-11,12-didehydroandrographolide regulated 48 proteins in which 21 were downregulated and 27 were upregulated. The list of regulated proteins with their probable activity and inactivity of both compounds is summarized in Table 1.

Enrichment analysis

Seventy-two different pathways were identified to be regulated by the Andrographolide in which pathways in cancer wereprimarily regulated by modulating nine genes i.e. AR, ESR2, IL6R, MDM2, PRKCA, RAC1, RARA, RHOA, RXRA at the false discovery rate of 4.96E-05. Similarly, 14-Deoxy-11,12-

didehydroandrographolide was predicted to regulate seventy-seven different pathways by modulating the Estrogen signaling pathway via seven genes i.e. ESR2, FKBP5, KRT16, KRT17, KRT18, PGR, RARA at the false discovery rate of 7.57E-06. Pathways modulated by Andrographolide and 14-Deoxy-11,12-didehydroandrographolide with their respective genes are summarized in Table 2 and Table 3 respectively.Similarly, the interaction of both compounds with the proteins from regulated pathways is represented in Figures 1 and 2. Further, the number of genes in multiple cellular components, biological process, and molecular function is for Andrographolide and 14-Deoxy-11,12-didehydroandrographolide are represented in Figure 3 and Figure 4, respectively. Similarly, network analysis of 14-Deoxy-11,12-didehydroandrographolide identified prime regulation of PRKCA protein and estrogen signaling pathway. Further, andrographolide primarily modulated PRKCA protein and pathways in cancer.

In silico molecular docking

Among Andrographolide and 14-Deoxy-11,12-didehydroandrographolide, 14-Deoxy-11,12-didehydroandrographolide was predicted to have the highest binding affinity with papain-like protease i.e. -6.7 kcal/mol; however, it was not having any hydrogen bond interactions. Similarly, andrographolide showed -6.5 kcal/mol binding energy with papain-like protein with one hydrogen bond interaction i.e. TYR274. Although both molecules were having equal binding energy with 3clpro (-6.8 kcal/mol), the number of hydrogen bond interactions were more in andrographolide due to interaction with THR190, HIS163, and CYS145. Further, both molecules showed a binding affinity with spike protein i.e. -6.9kcal/mol; however,andrographolide showed one hydrogen bond interaction with LYS807 (Table 4). The interaction of each compound with respective proteins is represented in Figure 5.

Drug-likeness and ADMET profiling

14-Deoxy-11,12-didehydroandrographolide scored higher druglikeness score i.e. -0.52 compared to andrographolide which was computed based on molecular weight, number of hydrogen bond donor, number of hydrogen bond acceptor and LogP value (Table 5) which has influenced the pharmacokinetic characters of both compounds by affecting absorption, distribution, metabolism, excretion, and toxicity (Figure 6).

Discussion

The present study dealt to investigate one of the active biomolecules andrographolide and its derivative 14-Deoxy-11,12-didehydroandrographolide from *Andrographis paniculata* to modulate the proteins/pathways for immunomodulatory activity and their binding affinity with three proteins i.e. 3clpro, PLpro and spike protein which are the targets of COVID infection. Further, we investigated the drug-likeness character of both molecules in which andrographolide scored lower drug-likeness character compared to its derivative. However, on looking to the binding affinity and number of hydrogen bond interactions, andrographolide showed a higher affinity towards the selected targets. This suggests, fewer modifications could be made in the andrographolide moiety to enhance the drug-likeness character without altering the binding affinity of the molecules.

Subjects with lower immunity systems are identified to be more prone towards the infection with COVID 19 due to compromised immunity systems (Science daily, 2020) which can be well visualized in the subjects who are suffering from an infectious and non-infectious disease. In this case, it is important to enhance the immunity of the subjects to minimize the probability of viral infection. In the present study via the enrichment analysis, we identified pathways that are involved to boost the immune system which is modulated by andrographolide and its derivative.

In the present study, we identified modulation of few pathways that are directly or indirectly linked with the modulation of the immune system i.e. Chemokine signaling pathway, Rap1 signaling pathway, Cytokine-cytokine receptor interaction, MAPK signaling pathway, NF-kappa B signaling pathway, Rassignaling pathway, p53 signaling pathway, HIF-1 signaling pathway, and Natural killer cell-mediated cytotoxicity. Among the above pathways, Chemokine signaling pathways, Rap1 signaling pathway, and Cytokine-cytokine receptor interaction are the choice of interest pathways as they are directly linked with the modulation of the immune system and they scored minimum false discovery rate compared to rest of the pathways. Chemokine signaling pathway was found to be modulated by andrographolide and its derivative which could contribute to controlling the migration of immune cells in tissues (Sokol and Luster, 2015). Further, Rap1 signaling pathway is involved in activating three secondary messengers i.e. cAMP, calcium, and diacylglycerol (Kortlever et al., 2017) which are needed in the signaling of cell position during viral infections; modulated by andrographolide by regulating ID1, PRKCA, RAC1, RAP1A, and RHOA and by 14-deoxy-11,12-didehydroandrographolide by regulating FLT1, ID1, PRKCA, RAC1, RAP1A, and RHOA. Similarly, cytokine-cytokine receptor interaction has been recorded by the KEGG database as an entry (hsa04060) in various auto-immune disorders. Since COVID-19 has a more risk over the infections on altered immune system of subjects, modulation of this pathway could be beneficial in them which has been modulated by andrographolide and its derivative. Further, the MAPK signaling pathway has been identified to play important role in the functioning of T lymphocytes (Chi and Flavell, 2010), was observed to be modulated by andrographolide and its derivative. Additionally, other pathways like NF-kappa B signaling pathway, Rassignaling pathway, p53 signaling pathway, HIF-1 signaling pathway, and Natural killer cell-mediated cytotoxicity are also regulated which has been well reported to be involved in the modulation of the immune system.

In COVID-19 infection, the n-CoV-2 binds to ACE-2 and enters into the cell and starts deregulating the intracellular functions by altering the normal homeostatic stimulus (Magrone et al., 2020). Hence, it is needed to have control over the components by binding over them or responding towards the stimulus COVID-19 main protease, or at least to minimize its effect by controlling the intracellular cascade initiated by the viral infection. In the present study, GO enrichment analysis identified andrographolide and 14-Deoxy-11,12-didehydroandrographolide were also predicted to majorly target the intracellular components, binding capacity towards various proteins as a molecular function and responder towards stimulus which could be the probable action of these two agents over the viral infection.

A concept of modulation of multiple proteins by a single molecule is the choice of research interest in identifying the lead hit and their respective targets. Further, andrographolide has been previously reported

to possess anti-viral property (Gupta et al 2017). Hence, based on the same concept, andrographolide and its derivative may also possess the anti-viral efficacy over COVID-19 which kindled us evaluating the binding affinity of these bioactives over andrographolidePLpro, 3clpro, and spike protein. Although the drug-likeness score model predicted 14-Deoxy-11,12-didehydroandrographolide to behave like a drug based on “Rule of Five”, its binding affinity and number of hydrogen bond interactions showed andrographolide to inhibit more on three proteins of COVID-19 i.e. Papain-like protease (PLpro), 3clpro, and spike protein.

Conclusion

The present study dealt to utilize the system biology approach to investigate the andrographolide and its derivative against COVID-19 by modulating the multiple pathways in which the Chemokine signaling pathway could be a choice of interest as it is directly linked to the modulation of the immune system with lowest false discovery rate. Further, andrographolide could possess higher importance compared to its derivate 14-Deoxy-11,12-didehydroandrographolide as it scored higher interaction with the targeted proteins of COVID-19.

Declarations

Competing interest: The authors declare no competing interest.

References

- Coronaviridae Study Group of the International Committee on Taxonomy of Viruses. The species severe acute respiratory syndrome-related coronavirus: classifying 2019-nCoV and naming it SARS-CoV-2. Nat Microbiol 2020; 5: 536-44.
- Bahmani M, Saki K, Shahsavari S, Rafieian-Kopaei M, Sepahvand R, Adineh A. Identification of medicinal plants effective in infectious diseases in Urmia, northwest of Iran. Asian Pac J Trop Biomed 2015; 5(10):858-64.
- Chen CJ, Michaelis M, Hsu HS, Tsai CC, Yang KD, Wu YC, Cinatl J, Doerr HW. ToonasinensisRoem tender leaf extract inhibits SARS coronavirus replication. J Ethnopharmacol 2008; 120:108-11.
- Chen JX, Xue HJ, Ye WC, Fang BH, Liu YH, Yuan SH, Yu P, Wang YQ. Activity of andrographolide and its derivatives against influenza virus in vivo and in vitro. Biol Pharm Bull 2009; 32(8):1385-91.
- Chi H, Flavell RA. Studies on MAP Kinase signaling in the immune system. Methods Mol Biol 2010; 661:471-80.
- Chikhale RV, Sinha SK, Patil RB, Prasad SK, Shrivastava SK, Shakya A, Gurav NS, Prasad RS. Gurav SS. SARS-CoV-2 host entry and replication inhibitors from Indian ginseng: in silico approach. J Biomole Stru Dyna 2020 (In Press https://doi.org/10.1080/07391102.2020.1778539).
- Churiyah, Pongtuluran OB, Rofaani E, Tarwadi. Antiviral and immunostimulant activities of *Andrographis paniculata.* HAYATI J Biosci 2015;22(2):67-72.

- Edwin ES, Vasantha-Srinivasan P, Senthil-Nathan S, Thanigaivel A, Ponsankar A, Pradeepa V, Selin-Rani S, Kalaivani K, Hunter WB, Abdel-Megeed A, Duraipandiyan V, Al-Dhabi NA. Anti-dengue efficacy of bioactive andrographolide from *Andrographis paniculata* (Lamiales: Acanthaceae) against the primary dengue vector Aedes aegypti (Diptera: Culicidae). Acta Trop 2016;163:167-78.
- Gupta S, Mishra KP, Ganju L. Broad-spectrum antiviral properties of andrographolide. Arch Virol 2017;162(3):611-23.
- Huang C, Wang Y, Li X, Ren L, Zhao J, Hu Y, Zhang L, Fan G, Xu J, Gu X, Cheng Z, Yu T, Xia J, Wei Y, Wu W, Xie X, Yin W, Li H, Liu M, Xiao Y, Gao H, Guo L, Xie J, Wang G., Rongmeng Jiang 3, Zhancheng Gao 13, Qi Jin 4, Jianwei Wang 14, Bin Cao. Clinical features of patients infected with 2019 novel coronavirus in Wuhan, China. Lancet 2020; 395: 497–506.
- Kortlever RM, Sodir NM, Wilson CH, Burkhart DL, Pellegrinet L, Swigart LB, Littlewood TD, Evan GI. Myc Cooperates with Ras by Programming Inflammation and Immune Suppression. Cell 2017;171(6):1301-15.e14.
- Lagunin A, Ivanov S, Rudik A, Filimonov D, Poroikov V. DIGEP-Pred: web service for in silico prediction of drug-induced gene expression profiles based on structural formula. Bioinformatics 2013;29(16):2062-3.
- Lee JC, Tseng CK, Young KC, Sun HY, Wang SW, Chen WC, Lin CK, Wu YH. Andrographolide exerts anti-hepatitis C virus activity by up-regulating haeme oxygenase-1 via the p38 MAPK/Nrf2 pathway in human hepatoma cells. Br J Pharmacol 2014; 171(1):237-52.
- Lin CW, Tsai FJ, Tsai CH, Lai CC, Wan L, Ho TY, Hsieh CC, Chao PD. Anti-SARS coronavirus 3C-like protease effects of Isatisindigotica root and plant-derived phenolic compounds. Antiviral Research 2005; 68:36-42
- Lin TP, Chen SY, Duh PD, Chang LK, Liu YN. Inhibition of the Epstein-barr virus lytic cycle by andrographolide. Biol Pharm Bull; 2008 31:2018-23.
- Magrone T, Magrone M, Jirillo E. Focus on receptors for coronaviruses with special reference to angiotensin-converting enzyme 2 as a potential prug target - A perspective. Endocr Metab Immune Disord Drug Targets. 2020.
- Mahady GB. Medicinal plants for the prevention and treatment of bacterial infections. Curr Pharm Des 2005; 11(19):2405-27.
- Mishra K, Dash AP, Dey N. Andrographolide: A novel antimalarial diterpene lactone compound from *Andrographis paniculata* and its interaction with curcumin and artesunate. J Trop Med 2011; 2011:579518.
- Mopuri R, Ganjayi M, Banavathy KS, Parim BN, Meriga B. Evaluation of anti-obesity activities of ethanolic extract of *Terminalia paniculata* bark on high fat diet-induced obese rats. BMC Complement Altern Med 2015; 15:76.
- Morris GM, Huey R, Lindstrom W, Sanner MF, Belew RK, Goodsell DS, Olson AJ. AutoDock4 and AutoDockTools4: Automated docking with selective receptor flexibility. J Comput Chem 2009; 30(16):2785-91.

- Opitz B, van Laak V, Eitel J, Suttorp N. Innate immune recognition in infectious and noninfectious diseases of the lung. Am J RespirCrit Care Med 2010; 181(12):1294–1309.
- Pongtuluran OB, Rofaani E. Antiviral and immunostimulant activities of *Andrographis paniculata*. HAYATI J Biosci. 2015 Apr 1;22(2):67-72.
- Puri A, Saxena RP, Saxena KC, Srivastava V, Tandon JS. Immunostimulating agents from *Andrographis paniculata*. J Nat Prod 1993; 56:995-9.
- Ryu YB, Jeong HJ, Kim JH, Kim YM, Park JY, Kim D, Nguyen TT, Park SJ, Chang JS, Park KH, Rho MH, Lee WS. Biflavonoids from *Torreya nucifera* displaying SARS-CoV 3CL(pro) inhibition. Bioorganic & Medicinal Chemistry 2010; 18, 7940-47
- Schwede T, Kopp J, Guex N, Peitsch MC. SWISS-MODEL: An automated protein homology-modeling server. Nucleic Acids Res. 2003;31(13):3381-5.
- Science daily. COVID-19: The immune system can fight back. [Internet] Available at: https://www.sciencedaily.com/releases/2020/03/200317103815.htm. Accessed on: 27-May-2020
- Seniya C, Shrivastava S, Singh SK, Khan GJ. Analyzing the interaction of a herbal compound Andrographolide from *Andrographis paniculata* as a folklore against swine flu (H1N1). Asian Pac J Trop Dis 2014; 4(Suppl 2): S624-30.
- Sinha SK, Prasad SK, Gurav SS, Patil RB,...ShakyaA. Identification of Bioactive Compounds from *Glycyrrhiza glabra* as Possible Inhibitor of SARS-CoV-2 Spike Glycoprotein and Non-structural Protein-15: A Pharmacoinformatics Study. J Biomole Stru Dyna 2020. (In press https://doi.org/10.1080/07391102.2020.1779132)
- Sinha, SK, Shakya A, Prasad S K, Singh S, Gurav N S, Prasad R S, Gurav SS. An *in-silico* evaluation of different Saikosaponins for their potency against SARS-CoV-2 using NSP15 and fusion spike glycoprotein as targets. J Biomole Stru Dyn 2020:1-13.
- Sofowora A, Ogunbodede E, Onayade A. The role and place of medicinal plants in the strategies for disease prevention. Afr J Tradit Complement Altern Med. 2013;10(5):210-229.
- Sokol CL, Luster AD. The chemokine system in innate immunity. Cold Spring HarbPerspect Biol. 2015;7(5):a016303. DOI:10.1101/cshperspect.a016303
- Szklarczyk D, Morris JH, Cook H, et al. The STRING database in 2017: quality-controlled protein-protein association networks, made broadly accessible. Nucleic Acids Res. 2017; 45(D1):D362-D368.
- Wan S, Yi Q, Fan S, et al. Characteristics of lymphocyte subsets and cytokines in peripheral blood of 123 hospitalized patients with 2019 novel coronavirus pneumonia (NCP). medRxiv 2020; DOI:10.1101/2020.02.10.20021832 (preprint).
- Wang D, Hu B, Hu C, et al. Clinical characteristics of 138 hospitalized patients with 2019 novel coronavirus–infected pneumonia in Wuhan, China. JAMA 2020; 323: 061-69.
- Wang W, Wang J, Dong SF, et al. Immunomodulatory activity of andrographolide on macrophage activation and specific antibody response. ActaPharmacol Sin. 2010;31(2):191-201. DOI:10.1038/aps.2009.205

- Wen CC, Shyur LF, Jan JT, Liang PH, Kuo CJ, Arulselvan P, … Yang, NS. Traditional Chinese medicine herbal extracts of Cibotiumbarometz, Gentianascabra, Dioscoreabatatas, Cassia tora, and Taxilluschinensis inhibit SARS CoV replication. J Trad Complement Med 2011; 1;1-41-50
- Wiart C, Kumar K, Yusof MY, Hamimah H, Fauzi ZM, Sulaiman M. Antiviral properties of ent-labdene diterpenes of *Andrographis paniculata* Nees, inhibitors of herpes simplex virus type I**.** Phytother Res 2005; 19:1069-1070.
- Wintachai P, Kaur P, Lee RCH, Ramphan S, Kuadkitkan A, Wikan N, Ubol S, Roytrakul S, Chu JJH, Smith DR. Activity of andrographolide against chikungunya virus infection. Sci Rep 5, 14179.
- Xu Z, Shi L, Wang Y, et al. Pathological findings of COVID-19 associated with acute respiratory distress syndrome. Lancet Respir Med. 2020; 8: 420–22.
- Yang H, Lou C, Sun L, et al. Admet SAR 2.0: web-service for prediction and optimization of chemical ADMET properties. Bioinformatics 2019;35(6):1067-69.
- Zhang XF, Tan BK. Anti-diabetic property of ethanolic extract of *Andrographis paniculata* in streptozotocin-diabetic rats. Acta Pharmacol Sin. 2000;21(12):1157-64.
- Zhu N, Zhang D, Wang W, Li X, Yang B, Song J, Zhao X, Huang B, Shi W, Lu R, Niu P, Zhan F, Ma X, Wang D, Xu W, Wu G, Gao GF, Tan W. A novel coronavirus from patients with pneumonia in China, 2019. N Engl J Med 2020; 382, 727-33.

Tables

Table 1: Regulated proteins by andrographolide and 14-Deoxy-11,12-didehydroandrographolide

andrographolide						14-Deoxy-11,12-didehydroandrographolide					
DownRegulation			UpRegulation			DownRegulation			UpRegulation		
Pa	Pi	Modulated proteins	Pa	Pi	Modulated proteins	Pa	Pi	Modulated proteins	Pa	Pi	Modulated proteins
0.548	0.132	TOP2A	0.589	0.131	VDR	0.66	0.117	CHEK1	0.701	0.077	VDR
0.559	0.163	CHEK1	0.526	0.082	CD14	0.627	0.097	TOP2A	0.599	0.043	CD14
0.387	0.028	KRT16	0.336	0.079	CLU	0.562	0.041	IVL	0.47	0.045	CLU
0.364	0.038	KRT17	0.444	0.198	AR	0.451	0.016	KRT16	0.548	0.124	AR
0.331	0.026	PTH	0.417	0.175	ID1	0.445	0.025	KRT17	0.522	0.161	CD83
0.394	0.138	ESR2	0.231	0.043	RAP1A	0.379	0.015	PTH	0.459	0.131	ID1
0.297	0.076	TIMP2	0.375	0.197	RAC1	0.452	0.092	ESR2	0.483	0.178	NPPB
0.38	0.161	CCL2	0.32	0.17	GPX1	0.474	0.127	MDM2	0.429	0.152	RAC1
0.38	0.161	IVL	0.241	0.092	KLK2	0.444	0.097	CCL2	0.41	0.134	SMN2
0.306	0.142	LEP	0.394	0.257	NPPB	0.34	0.044	TIMP2	0.39	0.124	TNFRSF1A
0.364	0.212	PRKCA	0.319	0.186	TNFRSF1A	0.357	0.086	LEP	0.262	0.027	RAP1A
0.3	0.155	CCL4	0.31	0.191	KRT18	0.403	0.139	PRKCA	0.362	0.129	KRT18
0.27	0.141	IL6R	0.171	0.058	RXRA	0.328	0.107	CCL4	0.325	0.096	CTSB
0.226	0.138	GYPA	0.356	0.248	RARA	0.382	0.187	NR3C1	0.35	0.124	GPX1
0.349	0.269	MDM2	0.205	0.103	RHOB	0.299	0.105	IL6R	0.287	0.077	KLK2
0.319	0.28	NR3C1	0.178	0.095	RHOA	0.384	0.206	CASP8	0.412	0.209	PLAT
0.221	0.206	CD44	0.354	0.328	CD83	0.139	0.051	PTHLH	0.397	0.211	RARA
			0.294	0.291	SMN2	0.247	0.166	CD44	0.371	0.201	CYP3A4
			0.191	0.19	CD38	0.362	0.293	NOS2	0.322	0.162	FKBP5
						0.276	0.229	FLT1	0.224	0.065	RHOB
						0.255	0.231	PROS1	0.195	0.04	RXRA
									0.2	0.057	RHOA
									0.231	0.094	CD38
									0.304	0.283	CAT
									0.243	0.226	PGR
									0.268	0.254	PLAU
									0.123	0.12	KRT7

Pa: probable activity, Pi: Probable inactivity

Table 2: Enrichment analysis of andrographolide

#term ID	term description	observed gene count	false discovery rate	matching proteins in network (labels)
hsa05200	Pathways in cancer	9	4.96E-05	AR,ESR2,IL6R,MDM2,PRKCA, RAC1,RARA,RHOA,RXRA
hsa04640	Hematopoietic cell lineage	5	7.61E-05	CD14,CD38,CD44,GYPA,IL6R
hsa04972	Pancreatic secretion	5	7.61E-05	CD38,PRKCA,RAC1,RAP1A, RHOA
hsa05130	Pathogenic Escherichia coli infection	4	0.00014	CD14,KRT18,PRKCA,RHOA
hsa04915	Estrogen signaling pathway	5	0.00016	ESR2,KRT16,KRT17,KRT18, RARA
hsa04932	Non-alcoholic fatty liver disease (NAFLD)	5	0.00022	IL6R,LEP,RAC1,RXRA, TNFRSF1A
hsa04062	Chemokine signaling pathway	5	0.00048	CCL2,CCL4,RAC1,RAP1A, RHOA
hsa05205	Proteoglycans in cancer	5	0.00059	CD44,MDM2,PRKCA,RAC1, RHOA
hsa04015	Rap1 signaling pathway	5	0.00063	ID1,PRKCA,RAC1,RAP1A, RHOA
hsa04670	Leukocyte transendothelial migration	4	0.00091	PRKCA,RAC1,RAP1A,RHOA
hsa04071	Sphingolipid signaling pathway	4	0.00095	PRKCA,RAC1,RHOA, TNFRSF1A
hsa04060	Cytokine-cytokine receptor interaction	5	0.0013	CCL2,CCL4,IL6R,LEP, TNFRSF1A
hsa04961	Endocrine and other factor-regulated calcium reabsorption	3	0.0013	KLK2,PRKCA,VDR
hsa05014	Amyotrophic lateral sclerosis (ALS)	3	0.0013	GPX1,RAC1,TNFRSF1A
hsa05418	Fluid shear stress and atherosclerosis	4	0.0013	CCL2,RAC1,RHOA, TNFRSF1A
hsa05206	MicroRNAs in cancer	4	0.0017	CD44,MDM2,PRKCA,RHOA
hsa04010	MAPK signaling pathway	5	0.0018	CD14,PRKCA,RAC1, RAP1A,TNFRSF1A
hsa04920	Adipocytokine signaling pathway	3	0.0024	LEP,RXRA,TNFRSF1A
hsa05152	Tuberculosis	4	0.0024	CD14,RHOA,TNFRSF1A,VDR
hsa05202	Transcriptional misregulation in cancer	4	0.0024	CD14,MDM2,RARA,RXRA
hsa05203	Viral carcinogenesis	4	0.0027	CHEK1,MDM2,RAC1,RHOA
hsa04151	PI3K-Akt signaling pathway	5	0.0031	IL6R,MDM2,PRKCA,RAC1, RXRA
hsa04510	Focal adhesion	4	0.0033	PRKCA,RAC1,RAP1A,RHOA
hsa05132	Salmonella infection	3	0.0035	CCL4,CD14,RAC1
hsa04064	NF-kappa B signaling pathway	3	0.0045	CCL4,CD14,TNFRSF1A
hsa04014	Ras signaling pathway	4	0.005	PRKCA,RAC1,RAP1A, RHOA
hsa04933	AGE-RAGE signaling pathway in diabetic complications	3	0.005	CCL2,PRKCA,RAC1
hsa04620	Toll-like receptor signaling pathway	3	0.0052	CCL4,CD14,RAC1
hsa04659	Th17 cell differentiation	3	0.0052	IL6R,RARA,RXRA
hsa04722	Neurotrophin signaling pathway	3	0.0067	RAC1,RAP1A,RHOA
hsa04919	Thyroid hormone signaling pathway	3	0.0067	MDM2,PRKCA,RXRA
hsa04310	Wnt signaling pathway	3	0.0116	PRKCA,RAC1,RHOA
hsa04150	mTOR signaling pathway	3	0.0124	PRKCA,RHOA,TNFRSF1A
hsa04921	Oxytocin signaling pathway	3	0.0124	CD38,PRKCA,RHOA
hsa04530	Tight junction	3	0.0161	RAC1,RAP1A,RHOA

hsa05144	Malaria	2	0.0161	CCL2,GYPA
hsa05164	Influenza A	3	0.0161	CCL2,PRKCA,TNFRSF1A
hsa04360	Axon guidance	3	0.0166	PRKCA,RAC1,RHOA
hsa04024	cAMP signaling pathway	3	0.0221	RAC1,RAP1A,RHOA
hsa04370	VEGF signaling pathway	2	0.0221	PRKCA,RAC1
hsa05169	Epstein-Barr virus infection	3	0.0221	CD38,CD44,MDM2
hsa04720	Long-term potentiation	2	0.0233	PRKCA,RAP1A
hsa04810	Regulation of actin cytoskeleton	3	0.0233	CD14,RAC1,RHOA
hsa05131	Shigellosis	2	0.0233	CD44,RAC1
hsa01524	Platinum drug resistance	2	0.0237	MDM2,TOP2A
hsa04115	p53 signaling pathway	2	0.0237	CHEK1,MDM2
hsa04520	Adherens junction	2	0.0237	RAC1,RHOA
hsa04664	Fc epsilon RI signaling pathway	2	0.0237	PRKCA,RAC1
hsa05100	Bacterial invasion of epithelial cells	2	0.0237	RAC1,RHOA
hsa05211	Renal cell carcinoma	2	0.0237	RAC1,RAP1A
hsa05214	Glioma	2	0.0237	MDM2,PRKCA
hsa05221	Acute myeloid leukemia	2	0.0237	CD14,RARA
hsa05223	Non-small cell lung cancer	2	0.0237	PRKCA,RXRA
hsa04918	Thyroid hormone synthesis	2	0.0239	GPX1,PRKCA
hsa05133	Pertussis	2	0.024	CD14,RHOA
hsa01521	EGFR tyrosine kinase inhibitor resistance	2	0.026	IL6R,PRKCA
hsa04350	TGF-beta signaling pathway	2	0.0287	ID1,RHOA
hsa05210	Colorectal cancer	2	0.0295	RAC1,RHOA
hsa04970	Salivary secretion	2	0.0297	CD38,PRKCA
hsa04666	Fc gamma R-mediated phagocytosis	2	0.0311	PRKCA,RAC1
hsa05146	Amoebiasis	2	0.0339	CD14,PRKCA
hsa01522	Endocrine resistance	2	0.034	ESR2,MDM2
hsa05215	Prostate cancer	2	0.0348	AR,MDM2
hsa04066	HIF-1 signaling pathway	2	0.0349	IL6R,PRKCA
hsa05231	Choline metabolism in cancer	2	0.0349	PRKCA,RAC1
hsa05142	Chagas disease (American trypanosomiasis)	2	0.0358	CCL2,TNFRSF1A
hsa04668	TNF signaling pathway	2	0.0399	CCL2,TNFRSF1A
hsa04270	Vascular smooth muscle contraction	2	0.047	PRKCA,RHOA
hsa04110	Cell cycle	2	0.0492	CHEK1,MDM2
hsa04380	Osteoclast differentiation	2	0.0492	RAC1,TNFRSF1A
hsa04611	Platelet activation	2	0.0492	RAP1A,RHOA
hsa04650	Natural killer cell mediated cytotoxicity	2	0.0492	PRKCA,RAC1

Table 3: Enrichment analysis of 14-deoxy-11,12-didehydroandrographolide

#term ID	term description	observed gene count	false discovery rate	matching proteins in network
hsa04915	Estrogen signaling pathway	7	7.57E-06	ESR2,FKBP5,KRT16,KRT17, KRT18,PGR,RARA
hsa05200	Pathways in cancer	11	7.57E-06	AR,CASP8,ESR2,IL6R, MDM2,NOS2,PRKCA,RAC1, RARA,RHOA,RXRA
hsa05202	Transcriptional misregulation in cancer	7	1.32E-05	CD14,FLT1,MDM2,PLAT,PLAU, RARA,RXRA
hsa04932	Non-alcoholic fatty liver disease (NAFLD)	6	9.13E-05	CASP8,IL6R,LEP,RAC1,RXRA, TNFRSF1A
hsa04972	Pancreatic secretion	5	0.00016	CD38,PRKCA,RAC1,RAP1A, RHOA
hsa05152	Tuberculosis	6	0.00016	CASP8,CD14,NOS2,RHOA, TNFRSF1A,VDR
hsa04015	Rap1 signaling pathway	6	0.00023	FLT1,ID1,PRKCA,RAC1,RAP1A, RHOA
hsa05014	Amyotrophic lateral sclerosis (ALS)	4	0.00023	CAT,GPX1,RAC1,TNFRSF1A
hsa05130	Pathogenic Escherichia coli infection	4	0.00023	CD14,KRT18,PRKCA,RHOA
hsa05205	Proteoglycans in cancer	6	0.00023	CD44,MDM2,PLAU,PRKCA,RAC1, RHOA
hsa05418	Fluid shear stress and atherosclerosis	5	0.00035	CCL2,PLAT,RAC1,RHOA, TNFRSF1A
hsa05206	MicroRNAs in cancer	5	0.00054	CD44,MDM2,PLAU,PRKCA, RHOA
hsa04060	Cytokine-cytokine receptor interaction	6	0.00065	CCL2,CCL4,FLT1,IL6R,LEP, TNFRSF1A
hsa04610	Complement and coagulation cascades	4	0.00065	CLU,PLAT,PLAU,PROS1
hsa05132	Salmonella infection	4	0.00075	CCL4,CD14,NOS2,RAC1
hsa04010	MAPK signaling pathway	6	0.00095	CD14,FLT1,PRKCA,RAC1, RAP1A,TNFRSF1A
hsa04062	Chemokine signaling pathway	5	0.00095	CCL2,CCL4,RAC1,RAP1A,RHOA
hsa04064	NF-kappa B signaling pathway	4	0.00095	CCL4,CD14,PLAU,TNFRSF1A
hsa04066	HIF-1 signaling pathway	4	0.00095	FLT1,IL6R,NOS2,PRKCA
hsa04640	Hematopoietic cell lineage	4	0.00095	CD14,CD38,CD44,IL6R
hsa05203	Viral carcinogenesis	5	0.00095	CASP8,CHEK1,MDM2,RAC1, RHOA
hsa05215	Prostate cancer	4	0.00095	AR,MDM2,PLAT,PLAU
hsa04510	Focal adhesion	5	0.00097	FLT1,PRKCA,RAC1,RAP1A, RHOA
hsa04620	Toll-like receptor signaling pathway	4	0.00097	CASP8,CCL4,CD14,RAC1
hsa05142	Chagas disease (American trypanosomiasis)	4	0.00097	CASP8,CCL2,NOS2,TNFRSF1A
hsa04670	Leukocyte transendothelial migration	4	0.0013	PRKCA,RAC1,RAP1A,RHOA
hsa04071	Sphingolipid signaling pathway	4	0.0014	PRKCA,RAC1,RHOA,TNFRSF1A
hsa04151	PI3K-Akt signaling pathway	6	0.0014	FLT1,IL6R,MDM2,PRKCA, RAC1,RXRA
hsa04014	Ras signaling pathway	5	0.0015	FLT1,PRKCA,RAC1,RAP1A, RHOA
hsa04961	Endocrine and other factor-regulated calcium reabsorption	3	0.0015	KLK2,PRKCA,VDR
hsa04115	p53 signaling pathway	3	0.004	CASP8,CHEK1,MDM2
hsa04920	Adipocytokine signaling pathway	3	0.004	LEP,RXRA,TNFRSF1A
hsa01524	Platinum drug resistance	3	0.0041	CASP8,MDM2,TOP2A

hsa04621	NOD-like receptor signaling pathway	4	0.0041	CASP8,CCL2,CTSB,RHOA
hsa05133	Pertussis	3	0.0045	CD14,NOS2,RHOA
hsa05146	Amoebiasis	3	0.0085	CD14,NOS2,PRKCA
hsa04933	AGE-RAGE signaling pathway in diabetic complications	3	0.0093	CCL2,PRKCA,RAC1
hsa04659	Th17 cell differentiation	3	0.0101	IL6R,RARA,RXRA
hsa04668	TNF signaling pathway	3	0.0115	CASP8,CCL2,TNFRSF1A
hsa05145	Toxoplasmosis	3	0.0115	CASP8,NOS2,TNFRSF1A
hsa04215	Apoptosis - multiple species	2	0.0127	CASP8,TNFRSF1A
hsa04722	Neurotrophin signaling pathway	3	0.0127	RAC1,RAP1A,RHOA
hsa04919	Thyroid hormone signaling pathway	3	0.0127	MDM2,PRKCA,RXRA
hsa04210	Apoptosis	3	0.0188	CASP8,CTSB,TNFRSF1A
hsa04310	Wnt signaling pathway	3	0.0215	PRKCA,RAC1,RHOA
hsa04150	mTOR signaling pathway	3	0.0231	PRKCA,RHOA,TNFRSF1A
hsa04921	Oxytocin signaling pathway	3	0.0231	CD38,PRKCA,RHOA
hsa04530	Tight junction	3	0.0306	RAC1,RAP1A,RHOA
hsa05134	Legionellosis	2	0.0306	CASP8,CD14
hsa05164	Influenza A	3	0.0306	CCL2,PRKCA,TNFRSF1A
hsa05416	Viral myocarditis	2	0.0308	CASP8,RAC1
hsa04360	Axon guidance	3	0.0311	PRKCA,RAC1,RHOA
hsa04370	VEGF signaling pathway	2	0.0327	PRKCA,RAC1
hsa04020	Calcium signaling pathway	3	0.0328	CD38,NOS2,PRKCA
hsa05168	Herpes simplex infection	3	0.0332	CASP8,CCL2,TNFRSF1A
hsa05167	Kaposi's sarcoma-associated herpesvirus infection	3	0.0335	CASP8,RAC1,TNFRSF1A
hsa05131	Shigellosis	2	0.0343	CD44,RAC1
hsa04720	Long-term potentiation	2	0.0347	PRKCA,RAP1A
hsa04024	cAMP signaling pathway	3	0.0362	RAC1,RAP1A,RHOA
hsa04664	Fc epsilon RI signaling pathway	2	0.0362	PRKCA,RAC1
hsa05169	Epstein-Barr virus infection	3	0.0362	CD38,CD44,MDM2
hsa05211	Renal cell carcinoma	2	0.0362	RAC1,RAP1A
hsa05214	Glioma	2	0.0362	MDM2,PRKCA
hsa05221	Acute myeloid leukemia	2	0.0362	CD14,RARA
hsa05223	Non-small cell lung cancer	2	0.0362	PRKCA,RXRA
hsa04520	Adherens junction	2	0.037	RAC1,RHOA
hsa04810	Regulation of actin cytoskeleton	3	0.037	CD14,RAC1,RHOA
hsa04918	Thyroid hormone synthesis	2	0.037	GPX1,PRKCA
hsa04976	Bile secretion	2	0.037	CYP3A4,RXRA
hsa05100	Bacterial invasion of epithelial cells	2	0.037	RAC1,RHOA
hsa01521	EGFR tyrosine kinase inhibitor resistance	2	0.0409	IL6R,PRKCA
hsa04146	Peroxisome	2	0.0433	CAT,NOS2
hsa04350	TGF-beta signaling pathway	2	0.0446	ID1,RHOA
hsa05323	Rheumatoid arthritis	2	0.045	CCL2,FLT1
hsa05210	Colorectal cancer	2	0.0454	RAC1,RHOA
hsa04970	Salivary secretion	2	0.0457	CD38,PRKCA
hsa04666	Fc gamma R-mediated phagocytosis	2	0.0481	PRKCA,RAC1

Table 4: Docking hits of andrographolide and 14-deoxy-11,12-didehydroandrographolide with Plpro, 3clpro and spike protein

Targets	Ligand	Binding Affinity (kcal/mol)	Number of hydrogen bonds	Hydrogen bond residues
Papain-like protease (PLpro) 7M0W	14-deoxy-11,12-didehydroandrographolide	-6.7	-	-
	andrographolide	-6.5	1	TYR274
3clpro 6LU7	14-deoxy-11,12-didehydroandrographolide	-6.8	1	ARG131
	andrographolide	-6.8	3	THR190,HIS163,CYS145
Spike protein	14-deoxy-11,12-didehydroandrographolide	-6.9	-	-
	andrographolide	-6.9	1	LYS807

Table 5: Druglikeness score of andrographolide and 14-deoxy-11,12-didehydroandrographolide

		andrographolide	14-deoxy-11,12-didehydroandrographolide
Molecular formula		$C_{20}H_{30}O_5$	$C_{20}H_{28}O_4$
Molecular weight		350.21	332.20
Number of HBA		5	4
Number of HBD		3	2
MolLogP		2.19	3.09
MolLogS	Log(moles/L)	-1.97	-2.67
	mg/L	3791.12	702.11
MolPSA (A^2)		71.27	55.16
MolVol (A^3)		416.03	421.79
Number of stereo centers		6	5
Drug-likeness model score		-0.64	-0.52

Figures

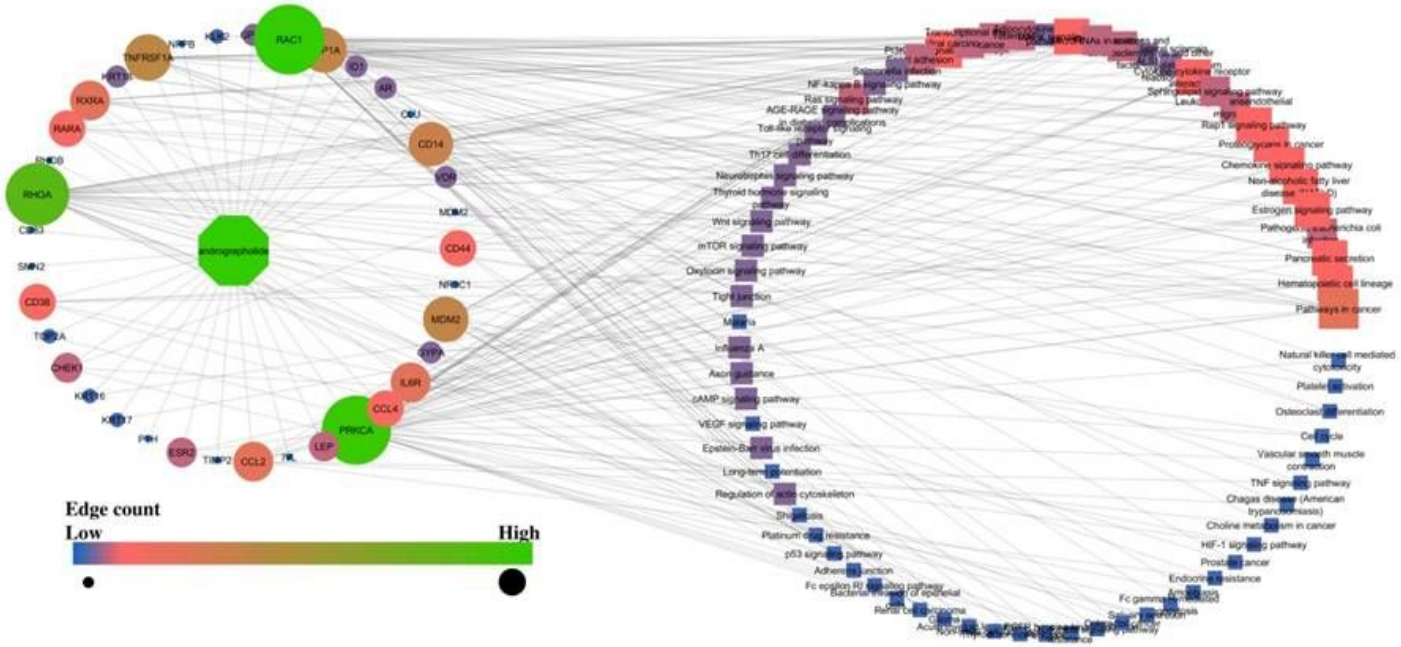

Figure 1

Network interaction of andrographolide with its targets and probably modulated pathways

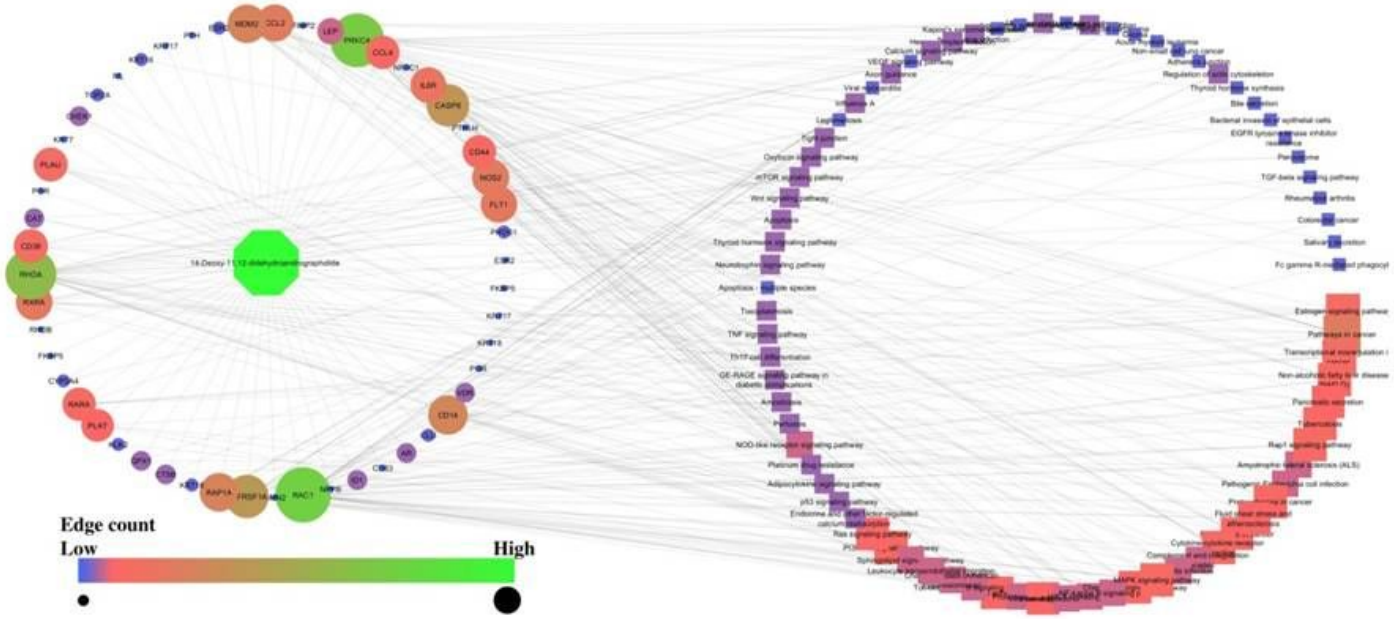

Figure 2

Network interaction of 14-Deoxy-11,12-didehydroandrographolide with its targets and probably modulated pathways

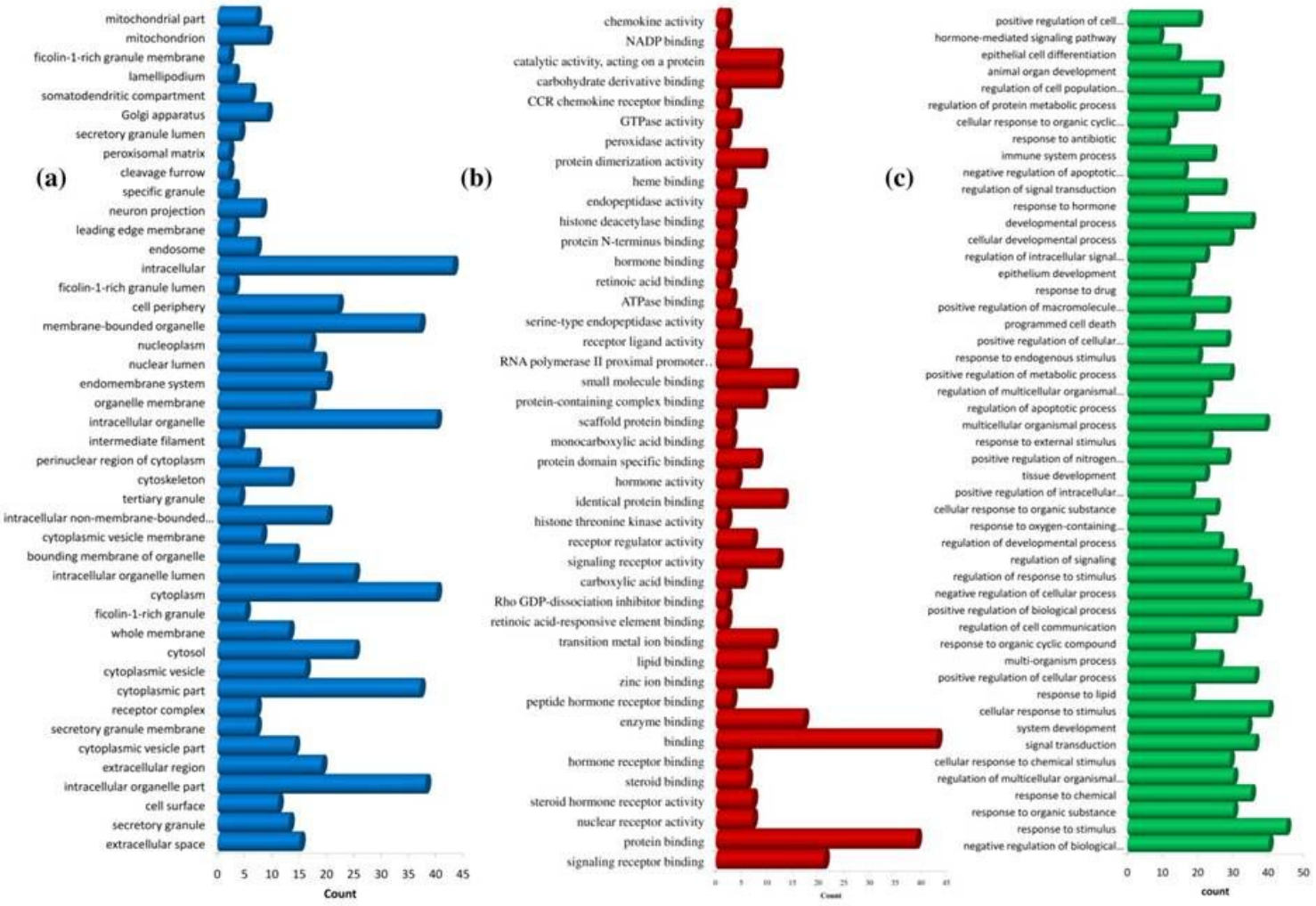

Figure 3

GO analysis for andrographolide (a) cellular component, (b) molecular function, and (c) biological process

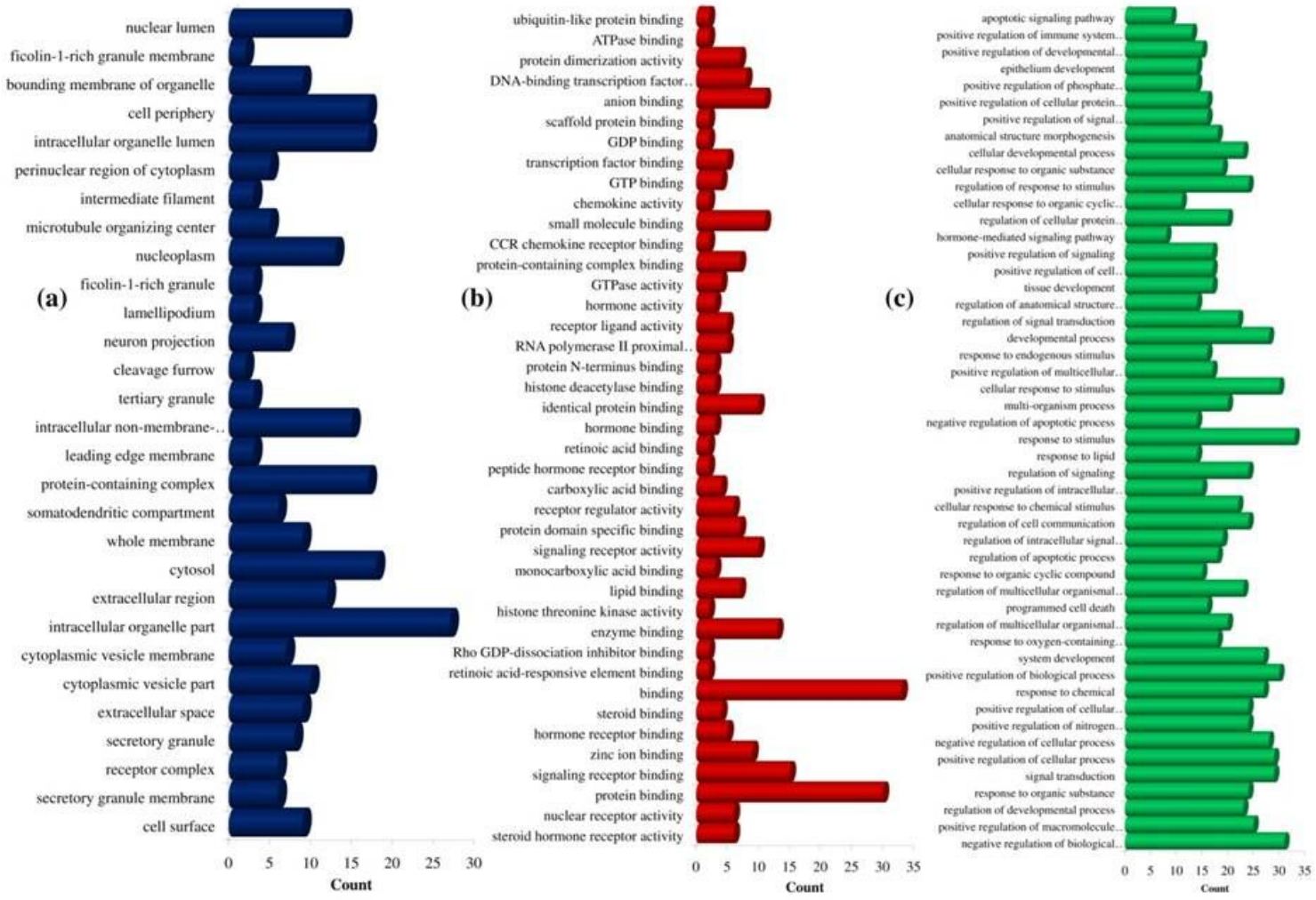

Figure 4

GO analysis for andrographolide (a) cellular component, (b) molecular function, and (c) biological process

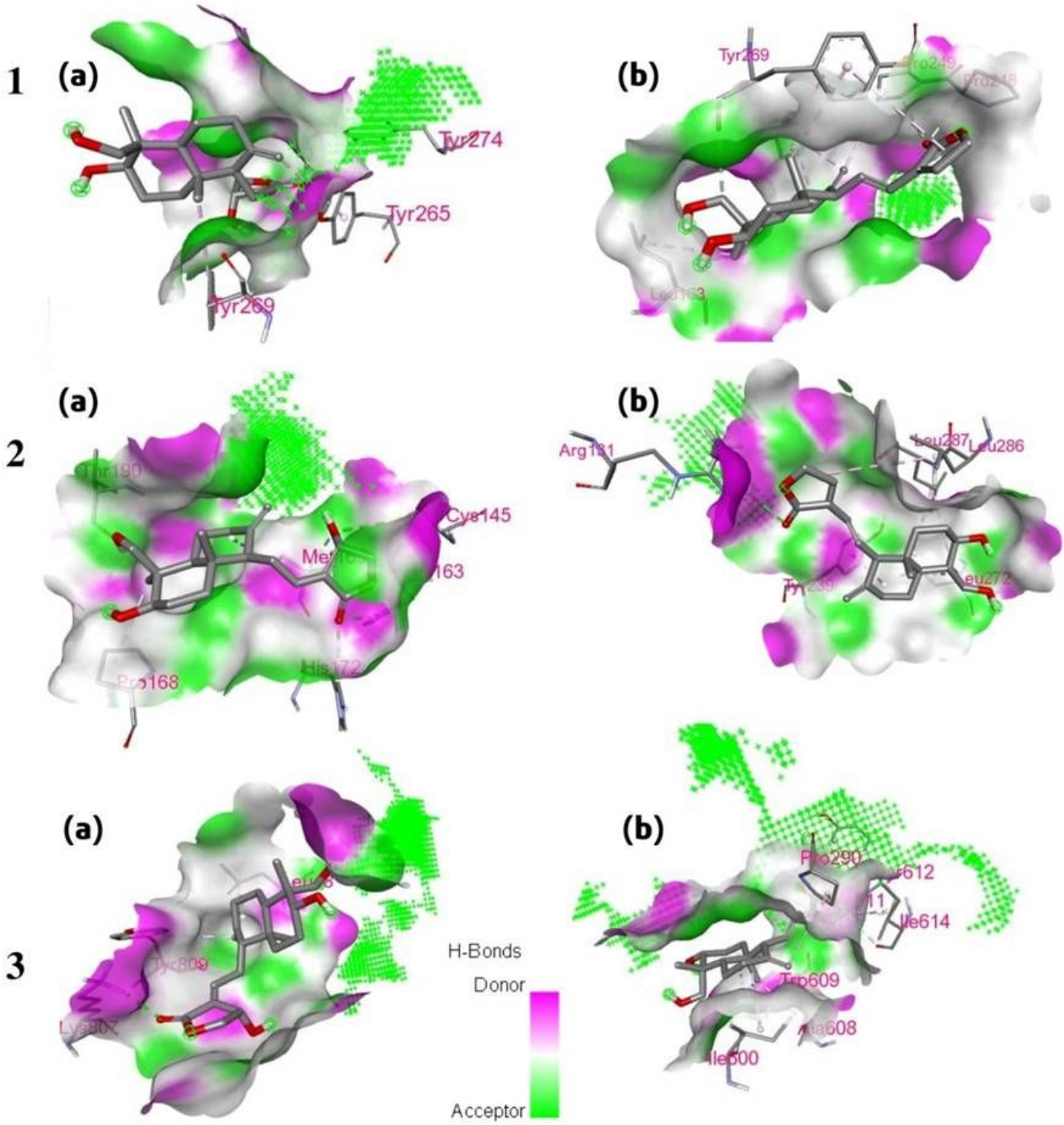

Figure 5

Interaction of (a) Andrographolide and (b) 14-Deoxy-11_12-didehydroandrographolide with (1) PLpro, (2)3clpro and (3) spike protein

	A	B
Human Intestinal Absorption	0.9822	0.9851
Caco-2	0.6206	0.6505
Human oral bioavailability	-0.6143	-0.6143
OATP2B1 inhibitior	-1	-1
OATP1B1 inhibitior	0.9414	0.9065
OATP1B3 inhibitior	0.948	0.9414
MATE1 inhibitior	-0.8412	-0.8812
Blood Brain Barrier	0.944	0.9064
P-glycoprotein inhibitior	-0.8095	-0.8149
P-glycoprotein substrate	-0.6948	-0.7405
CYP3A4 substrate	0.6897	0.6607
CYP2C9 substrate	-0.8075	-1
CYP2D6 substrate	-0.8784	-0.8817
CYP3A4 inhibition	-0.8309	-0.7701
CYP2C9 inhibition	-0.9071	-0.9135
CYP2C19 inhibition	-0.9025	-0.9029
CYP2D6 inhibition	-0.9326	-0.9317
CYP1A2 inhibition	-0.9046	-0.8936
UGT catelyzed	0.7	0.7
Eye corrosion	-0.991	-0.9907
Eye irritation	-0.8955	-0.9307
Ames mutagenesis	-0.62	-0.78
Human ether-a-go-go inhibition	-0.4917	-0.3798
micronuclear	-0.91	-0.91
Hepatotoxicity	-0.725	-0.75

Figure 6

ADMET (a) Andrographolide, (b) 14-Deoxy-11,12-didehydroandrographolide Red:lower, Green: High